Publication Year	2018
Acceptance in OA	2020-11-09T13:51:08Z
Title	Compact Dual-Polarization Cryogenic Receiver Module for the 75-116 GHz band
Authors	NAVARRINI, Alessandro, VALENTE, Giuseppe, Serres, Patrice, Schaefer, Franck, Thome, Fabian, Garnier, Olivier
Publisher's version (DOI)	10.1109/ICEAA.2018.8520415
Handle	http://hdl.handle.net/20.500.12386/28218

Compact Dual-Polarization Cryogenic Receiver Module for the 75-116 GHz band

Alessandro Navarrini
Astronomical Observatory of Cagliari
INAF
Selargius, Italy
alessandro.navarrini@inaf.it

Giuseppe Valente
ASI (Italian Space Agency)
Rome, Italy
giuseppe.valente@asi.it

Patrice Serres
Front-End Group
IRAM
Saint Martin d'Hères, France
serres@iram.fr

Frank Schaefer
Max-Planck Institute for Radio Astronomy
Bonn, Germany
fschaefer@mpifr-bonn.mpg.de

Fabian Thome
IAF (Fraunhofer Institute for Applied Solid State Physics IAF)
Freiburg, Germany
Fabian.Thome@iaf.fraunhofer.de

Olivier Garnier
Front-End Group
IRAM
Saint Martin d'Hères, France
garnier@iram.fr

***Abstract*—We describe the design of a highly integrated cryogenic receiver module based on an "active" waveguide Orthomode Transducer (OMT) for dual-polarization radio astronomy observations across 75-116 GHz (3-mm band). The receiver module consists of passive and active sections incorporated in three mechanical blocks arranged in a very compact assembly. The module has external dimensions of 43×25×35 mm^3; it includes a square waveguide input (size 2.54×2.54 mm^2) and two standard WR10 waveguide outputs (size 1.27×2.54 mm^2) parallel to the input waveguide, suitable for integration in a focal plane array.**

The passive section of the receiver module employs a broadband backward-coupler waveguide OMT while the active section consists of two ultra-low noise MMIC (Monolithic Microwave Integrated Circuit) amplifiers in cascade, delivering a total gain of ≈45 dB for each of the polarization channels. The "active OMT" receiver will be cryogenically cooled at the physical temperature of ≈15 K. It is expected to provide state-of-the-art performance with noise in the range 25 to 50 K across 75-116 GHz. The module incorporates a DC power supply board along with discrete capacitors, resistors and DC bias connector for biasing the MMIC amplifiers.

Keywords—Orthomode Transducer (OMT), MMIC, Low Noise Amplifier (LNA), integrated receiver, millimeter-wave radio astronomy.

I. Introduction

Orthomode Transducers are key components of dual-polarization receivers for radio astronomy [1]. An OMT has three physical ports but exhibits electrical properties of a four-port device. The input common port, usually a waveguide with a square or a circular cross-section, has two electrical ports carrying two orthogonal independent linearly polarized RF signals. Highly symmetric OMT structures allow achieving a full waveguide band with relative band ($\Delta\nu/\nu_c$) of over 50%. At microwave and millimeter wavelengths OMT configurations utilize planar [2-8], coaxial [9-10] or waveguide transmission lines. Typical waveguide OMT structures with relative bandwidth larger than ≈30% are based on Boifot junctions [11], turnstile junctions [12-15] or dual-ridge designs [16]. An OMT based on reverse-coupling waveguide junction was proposed in [17].

Here, we describe the design of a dual-polarization receiver module based on a waveguide OMT employing the broadband symmetrical reverse-coupling OMT structure presented in [18-19]. The OMT integrates MMIC LNAs (Low Noise Amplifiers,) designed and fabricated at IAF [20-21], and waveguide-to-microstrip transitions to be fabricated at IRAM.

This active waveguide OMT is developed in the framework of Work Package 1 of the AETHRA (Advanced European Technologies for Heterodyne Receiver for Astronomy) programme, aiming at investigating the new 35 nm gate length mHEMT (Metamorphic High Electron Mobility Transistor) technology for improving MMIC LNA performance.

Our goal is to develop a prototype of dual polarization 3×3 multibeam receiver array, based on the active waveguide OMT described here, and to install it on the focal plane of the IRAM 30-m radio telescope on Pico Veleta, Spain [22]. The integrated receiver array will be cooled at the physical temperature of ≈15 K provided by a commercial cryogenic refrigerator.

In section II we describe the architecture of the active OMT dual-polarization receiver. We discuss its electromagnetic and mechanical designs in sections III and IV, respectively.

II. Architecture of the Dual-Polarization Receiver Module

Fig. 1 shows a block diagram of the dual-polarization receiver module. The device consists of a "passive" OMT based on a backward coupler waveguide structure and of an "active" waveguide circuitry with MMIC LNAs packaged in a single mechanical module. The passive waveguide OMT utilizes a square input for connection to a dual-polarization feed-horn. The OMT separates the two orthogonal linearly polarized input signals in two independent waveguide outputs located inside the module. Each polarization signals is coupled to the "active" circuitry consisting of a cascade of two MMIC amplifiers through waveguide-to-microstrip transitions based on quartz substrate with Gold beam-lead interconnection. The two MMICs of each cascade are interconnected through a microstrip line fabricated on quartz and located inside a channel. The signals at the output of the second MMIC amplifier of the cascade is coupled back to waveguide through a microstrip-to-waveguide transition. Two amplified signals, one per polarization channel, are

This project has received funding from the European Union's Horizon 2020 research and innovation programme under grant agreement No 730562.

XXX-X-XXXX-XXXX-X/XX/$XX.00 ©20XX IEEE

available at the WR10 waveguide outputs of the receiver module (OMT output 1 and OMT output 2 – see Fig. 1).

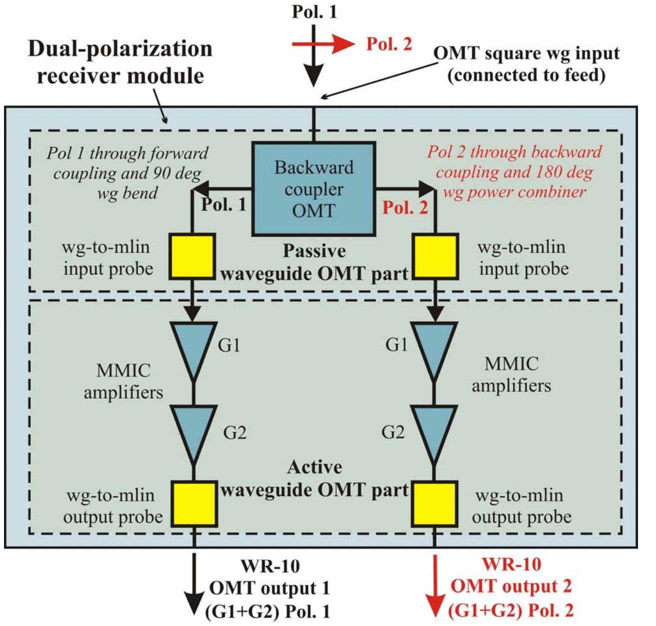

Fig. 1. Block diagram of dual-polarization receiver module based on a passive OMT part and on an active part integrating MMIC LNAs.

III. Design of Dual Polarization Receiver Module

A. *Passive waveguide OMT*

The network representation of the *symmetric* backward coupling waveguide structure used in the OMT is shown in Fig. 2. Here, Pol 1 and Pol 2 propagate through a common input port. Pol 1 signal is fully coupled to the straight output port *(4)*. Instead, Pol 2 signal at port (*1*) is equally split between two 90 hybrid couplers, whose output ports (*5*) and (*6*) are terminated with reactive loads. Thus, Pol 2 signal is backward-coupled at -3 dB to output ports (*2*) and (*3*) with a phase difference of 180 deg.

Fig. 3 shows the full 3D structure of the passive part of the waveguide OMT inner structure, consisting essentially of the dual-side backward coupler, of a 90 deg E-plane rectangular-to-oval waveguide bend transition for Pol 1, and

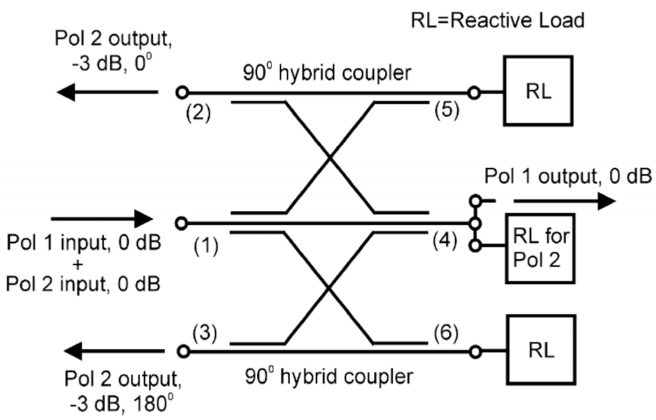

Fig. 2. Schematic representation of the ideal polarization splitting network (OMT) with forward coupling of Pol 1 from ports 1 to 4 and symmetric 3-dB backward coupling of Pol 2 from port 1 to ports 2 and 3. The structure consists of two 90⁰ hybrid couplers with reactively loaded (RL) outputs. Port 1 is in common to the two hybrids. Signals at ports 2 and 3, 180⁰ out-of-phase, are re-combined by a 180⁰ power combiner.

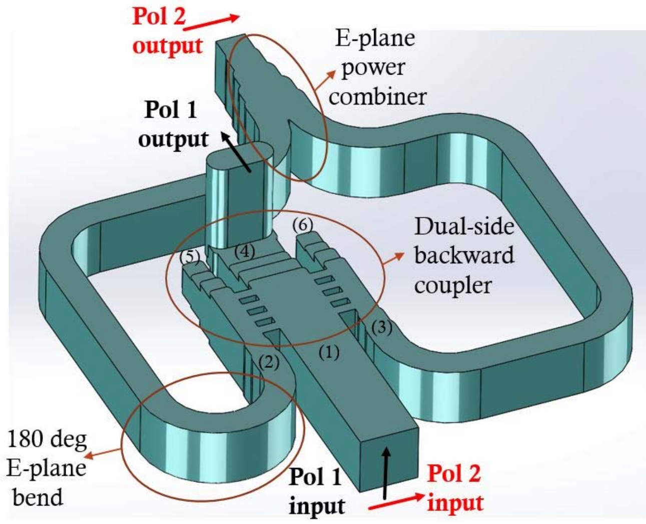

Fig. 3. 3D view of the OMT passive part showing the polarization splitting dual-side backward coupler, the two 180 deg and 90 deg E-plane bends, the E-plane power combiner, and the 90 deg E-plane bend transition. Numbers (1)-(6) inside or close the waveguides of the backward coupling structure refer to the port numbering adopted in the schematic of Fig. 2.

of one E-plane Y-junction power combiner for Pol 2. The position of the Pol 2 output rectangular waveguide is shifted with respect to the input square waveguide to allow integration of the MMICs (see next sub-section). The electrical lengths of the two sidearms between the backward coupler outputs and the power combiner inputs must be identical to guarantee that the Pol 2 signals recombine with the proper phase. Also, the electrical length of the square waveguide input must be minimized to reduce the cross-polarization that might be induced by possible mechanical misalignements between the two block halves of the passive part of the OMT (discussed further down, see Fig. 5). The full OMT was optimized using the commercial electromagnetic simulator CST Microwave Studio.

B. *Waveguide-to-microstrip transition*

The design of a parallel H-plane waveguide-to-microstrip transition employed in the dual-polarization module is shown in Fig. 4, left panel. The transition utilizes an antenna probe located on a 80 μm thick quartz chip (dielectric constant 3.8) housed in a channel 400 μm wide. The probe extends partially in the waveguide. The microstrip has a width of 120 μm. The conducting material of probe and microstrip is Gold, approximately 4 μm thick. A fix-tuned waveguide short-circuit located approximately a quarter wavelengths from the antenna probe provides a

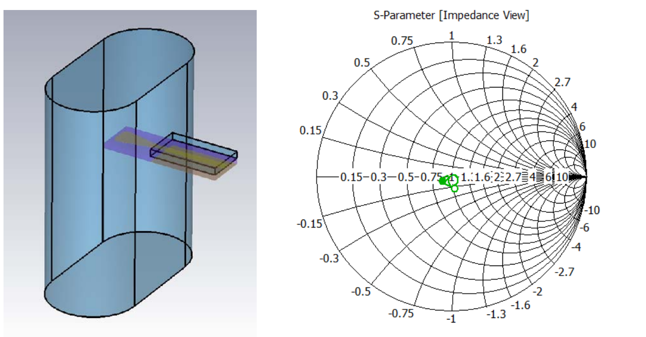

Fig. 4. Parallel H-plane waveguide-to-microstrip transitions employed in the dual polarization receiver module (left). Smith chart with simulation results of the transition across 75-116 GHz.

broadband response. The oval waveguide is matched to a standard WR10 waveguide (reflection coefficient greater than 37 dB). The result of the electromagnetic simulation of the optimized transition is shown on the Smith chart of Fig. 4, right panel. A reflection coefficient greater than 23 dB is obtained across the 75-116 GHz band.

C. *Full dual-polarization receiver module*

Fig. 5 shows the design of the dual-polarization receiver module equivalent to the architecture of Fig. 1. The inner structure of the module incorporates the passive waveguide backward coupler OMT (presented in section III-A), the waveguide-to-microstrip transitions (presented in section III B) and the cascade of the MMIC amplifiers. Sections of standard WR10 waveguides are used to route the signals amplified by the MMICs to suitable positions at the output of the module. The waveguide outputs are parallel and in-line with the waveguide input.

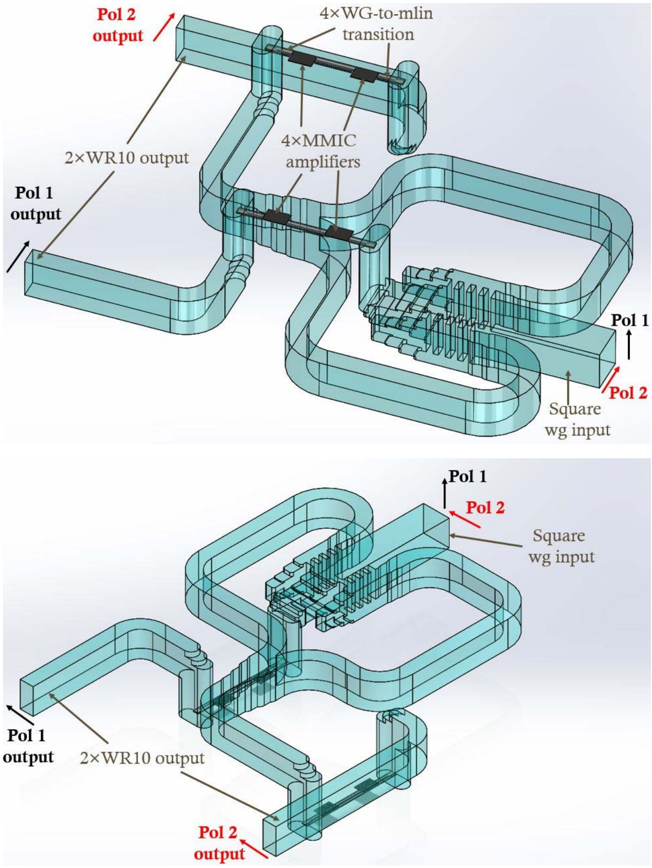

Fig. 5. Two different 3D views of the inner part of the dual-polarization receiver module showing the passive and active waveguide OMT parts, including the waveguide circuitries and the MMIC amplifiers.

IV. MECHANICAL DESIGN

The mechanical design of the dual-polarization module is presented in Fig. 6. The module consists of three mechanical blocks assembled in a compact unit with external dimension 43×25×35 mm^3. The waveguide circuitry of the OMT passive part is entirely implemented in "Block 2" and "Block 3", while the active part is incorporated in "Block 1". We note that the distance between the WR10 waveguides at the output of the module allows placing two standard UG387 flanges side-by-side

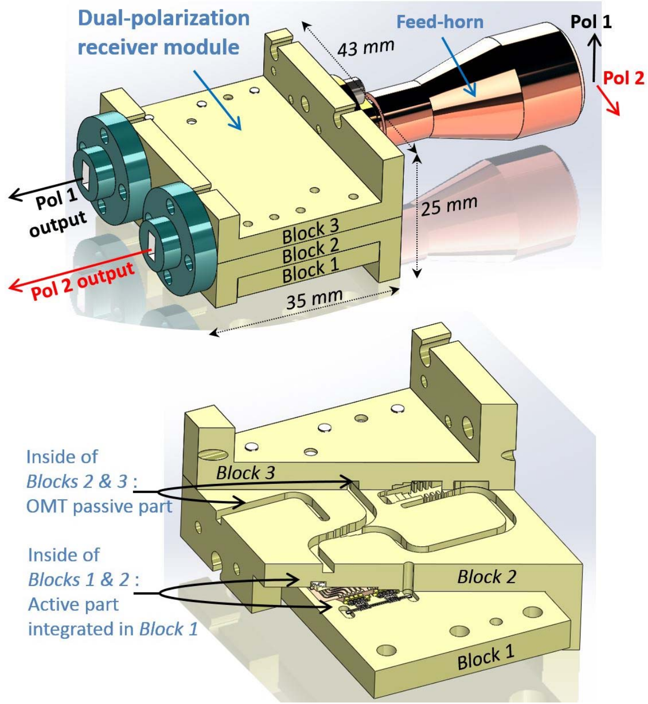

Fig. 6. 3D view of the dual-polarization receiver module. Top: fully assembled module with a feed-horn mounted at its input and two UG387 flanges mounted at its output to demonstrate its mechanical compatibility with external components. Bottom: cross-cut of the module showing the inner waveguide circuitry of the backward-coupler OMT implemented in Blocks 2 & 3 and the active part incorporated in Block 1.

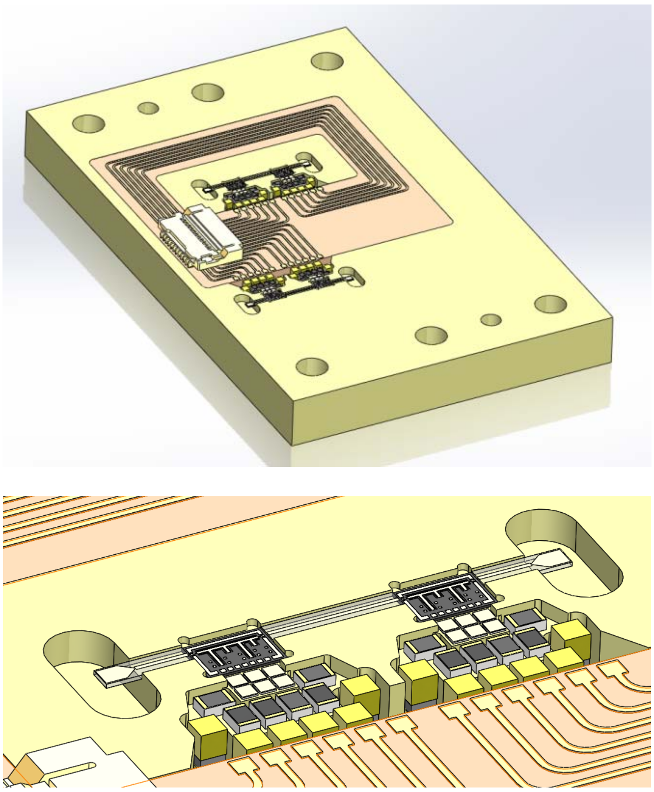

Fig. 7. 3D view of Block 1 (top) showing the packaging details of the MMICs with the waveguide-microstrip transitions and the bias circuitries, which include discrete capacitors and resistors (bottom).

(flange diameter 0.75 inch). In particular, the module width of 43 mm is compatible with the footprint dimension and distance between the axis of the feed-horns of the multibeam array, of about 45 mm. It would be possible to reduce the module width by re-routing the inner waveguide circuitries and by adopting non-standard output waveguide flanges.

Fig. 7 shows the mechanical design of Block 1 and the packaging details of the MMICs and of their bias circuitry. Flat flexible connector and cables are employed for distributing the DC bias to the LNAs.

REFERENCES

[1] J. D. Kraus, “Radio Astronomy”, McGraw-Hill Book Company, 1966.

[2] R. W. Jackson, "A planar orthomode transducer", *IEEE Microw. Wireless Compon. Lett.*, vol. 11, no. 12, pp. 483-485, Dec. 2001.

[3] G. Engargiola and R. L. Plambeck, “Tests of a planar L-band orthomode transducer in circular waveguide,” *Review of Scientific Instruments*, vol. 74, no. 3, p. 1380, 2003.

[4] P.K. Grimes, O.G. King, G. Yassin, M.E. Jones, “Compact broadband planar orthomode transducer,” *Electronics Letters*, Vol. 43 No. 2, 11th October 2007.

[5] S. Shu, S. Sekiguchi, M. Sekine, Y. Sekimoto, T. Nitta, A. Dominjon, T. Noguchi, M. Naruse, W. Shan, “Development of octave-band planar ortho-mode transducer with kinetic inductance detector for LiteBIRD,” *Proc. SPIE 9914, Millimeter, Submillimeter, and Far-Infrared Detectors and Instrumentation for Astronomy VIII*, 99142C 19 July, 2016.

[6] A. Navarrini, R. L. Plambeck, “Orthomode Transducers for Millimeter Wavelengths,” *Proceedings of URSI North American Radio Science Meeting*, invited, Ottawa, Canada, July 22-26, 2007.

[7] G. Valente, A. Navarrini, “Design of Planar Orthomode Transducer for 84-116 GHz,” *Proceedings of 24th International Symposium on Space Terahertz Technology*, Groningen, The Netherlands, 8-10 Apr 2013.

[8] G. Valente, A. Navarrini, F. Schaefer, P. Serres, F. Thome, “Architecture of Highly-Integrated Cryogenic Active Planar OMT for the 3 mm Band,” *Proceedings of the 2nd URSI-AT-RASC Conference*, Grand Canaria, May 28-June 2nd, 2018.

[9] G. Engargiola, A. Navarrini, “K-band orthomode transducer with waveguide ports and balanced coaxial probes,” *IEEE Trans. Microw. Theory Techn.*, vol. 53, n. 5, pp. 1792-1801, May 2005.

[10] G. Valente, G. Montisci, T. Pisanu, A. Navarrini, P. Marongiu, G. A. Casula, “A Compact L-Band Orthomode Transducer for Radio Astronomical Receivers at Cryogenic Temperature,” *IEEE Trans. Microw. Theory Tech*, vol. 63, no. 10, October 2015.

[11] A. M. Boifot, E. Lier, T. Schaug-Pettersen, “Simple and broadband orthomode transducer” *IEEE Proceedings*, Vol. 137, Pt. H, No. 6, December 1990, pp. 396-400.

[12] A. Navarrini and R.L. Plambeck, “A Turnstile Junction Waveguide Orthomode Transucer,” *IEEE Trans. Microwave Theory Tech.,* 54, n. 1, 272-277, 2006.

[13] A. Navarrini, R. L. Plambeck and D. Chow, “A Turnstile Junction Waveguide Orthomode Transducer for the 1 mm Band,” *Proceedings of the 16th International Symposium on Space Terahertz Technology*, Gothenburg, Sweden, May 02-04, 2005.

[14] A. Navarrini, A. Bolatto, R. L. Plambeck, “Test of 1 mm Band Turnstile Junction Waveguide Orthomode Transducer,” *Proceedings of the 17th International Symposium on Space Terahertz Technology*, Paris, France, May 10-12, 2006.

[15] G. Pisano, L. Pietranera, et al. , “A Broadband WR10 Turnstile Junction Orthomode Transducer,” *IEEE Micr. Wireless Comp. Lett.*, Vol. 17, n. 4, Apr. 2007.

[16] A. Dunning, “Double Ridged Orthogonal Mode Transducer for the16-26 GHz Microwave Band”, *Proc. of the Workshop on the Applications of Radio Science*, February 20-22, 2002.

[17] O. A. Peverini, R. Tascone, G. Virone, A. Olivieri, R. Orta, “Orthomode Transducer for Millimeter-Wave Correlation Receivers,” *IEEE Trans. Microwave Theory Tech*., vol. 54, n.5, May 2006.

[18] A. Navarrini, R. Nesti, “Symmetric reverse-coupled waveguide orthomode transducerfor the 3mm band,” *IEEE Trans. Microw. Theory Tech.*, vol. 57, no. 1, pp. 80-88, Jan. 2009.

[19] A. Navarrini, R. Nesti, “Dual-side backward coupler waveguide orthomode transducer for the 3 mm band,” *Proc. of SPIE Astronomical Telescope and Instrumentation, Millimeter and Submillimeter Detectors and Instrumentation for Astronomy IV*, Vol. 7020, 70202M, Marseille, France, 23-28 June 2008.

[20] F. Thome, A. Leuther, J. D. Gallego, F. Schäfer, M. Schlechtweg, and O. Ambacher, “70--116-GHz LNAs in 35-nm and 50-nm Gate-Length Metamorphic HEMT Technologies for Cryogenic and Room-Temperature Operation,” *IEEE MTT-S Int. Microw. Symp. Dig.*, Jun. 2018, pp. 1495-1498.

[21] F. Thome, A. Leuther, H. Massler, M. Schlechtweg, and O. Ambacher, “Comparison of a 35-nm and a 50-nm Gate-Length Metamorphic HEMT Technology for Millimeter-Wave Low-Noise Amplifier MMICs,” *IEEE MTT-S Int. Microw. Symp. Dig*., Jun. 2017, pp. 752–755.

[22] J. W. M. Baars, B. G. Hooghoudt, P. G. Mezger, M. J. de Jonge, “The IRAM 30-m millimeter radio telescope on Pico Veleta, Spain,” *Astronomy and Astrophysics*, 175, pp. 319-326, 1987.